Characterization of Rose Bengal-N,N′-Dimethyl-4,4′-bipyridinium Complexes and Their Separation in Aqueous SiO2 Colloids: Photophysical Properties of Rose Bengal in the Microheterog...

ARTICLE *in* THE JOURNAL OF PHYSICAL CHEMISTRY · JULY 1992

Impact Factor: 2.78 · DOI: 10.1021/j100193a075

4 AUTHORS, INCLUDING:

Yoav Eichen
Technion - Israel Institute of Technology
108 PUBLICATIONS **3,479** CITATIONS
SEE PROFILE

Ernesto Joselevich
Weizmann Institute of Science
75 PUBLICATIONS **4,167** CITATIONS
SEE PROFILE

(27) Braslavsky, S. E.; Heihoff, K. In Scaiano, J. C. *Handbook of Organic Photochemistry I*; CRC Press, Inc.: Boca Raton, FL, 1989; pp 327-356.
(28) Oesterhelt, D.; Stoeckenius, W. *Methods Enzymol.* **1974**, *31A*, 667-678.
(29) Heihoff, K.; Braslavsky, S. E.; Schaffner, K. *Biochemistry* **1987**, *26*, 1422-1427.
(30) Atkinson, G. H.; Blanchard, D.; Lemaire, H.; Brack, T. L.; Hayashi, H. *Biophys. J.* **1989**, *55*, 263-274.
(31) Birge, R. R.; Cooper, T. M.; Lawrence, A. F.; Masthay, M. B.; Zhang, C. F.; Zidovetzki, R. *J. Am. Chem. Soc.* **1991**, *113*, 4327-4328.
(32) Bilmes, G. M.; Tocho, J. O.; Braslavsky, S. E. *J. Phys. Chem.* **1988**, *92*, 5958-5963.
(33) Bevington, P. R. *Data Reduction and Error Analysis for the Physical Sciences*; McGraw-Hill Book Company: New York, 1969.
(34) Oesterhelt, D.; Hess, B. *Eur. J. Biochem.* **1974**, *37*, 316-326.
(35) Trissl, H.-W. *Photochem. Photobiol.* **1990**, *51*, 793-818.
(36) We include a very valuable suggestion from a referee who pointed out that cryogenic photocalorimetry leads to lower values for the energy content than our room temperature photoacoustics. Following this suggestion, photocalorimetry monitors enthalpy storage in a fully equilibrated system whereas picosecond time resolved photoacoustic measurements are relevant to a non-equilibrated protein in which the chromophore has not transferred all of its excess energy to the protein and the protein has not transferred all its energy to the surrounding environment.

Characterization of Rose Bengal-*N*,*N*′-Dimethyl-4,4′-bipyridinium Complexes and Their Separation in Aqueous SiO_2 Colloids: Photophysical Properties of Rose Bengal in the Microheterogeneous System†

Itamar Willner,* Yoav Eichen, Ernesto Joselevich,

Institute of Chemistry, The Hebrew University of Jerusalem, Jerusalem 91904, Israel

and Arthur J. Frank

National Renewable Energy Laboratory, 1617 Cole Boulevard, Golden, Colorado 80401
(Received: January 23, 1992)

Rose Bengal, Rb^{2-}, forms crystalline 1:1 and 2:1:1 complexes with *N*,*N*′-dimethyl-4,4′-bipyridinium, MV^{2+}. In the 1:1 complex the two components are coplanar with charge neutralization within the complex structure. In the 2:1:1 complex, one MV^{2+} unit is intercalated between two Rb^{2-} units and the second MV^{2+} unit is positioned externally to this sandwich structure and acts in charge neutralization. In both complexes, electrostatic interactions, charge-transfer interactions, and π-interactions stabilize the intermolecular assemblies. In solution, Rb^{2-} and MV^{2+} form initially the 1:1 intermolecular complex $[Rb^{2-}\cdots MV^{2+}]$; $K_{a(298K)} = 9000 \pm 500$, $\Delta G^\circ = -22.56 \pm 1.1$ KJ·mol^{-1}, $\Delta H^\circ = -36.62 \pm 2$ KJ·mol^{-1}, and $\Delta S = -0.048 \pm 0.0025$ KJ·mol^{-1}·K^{-1}. In the presence of added silica colloid, the $[Rb^{2-}\cdots MV^{2+}]$ complex is separated through the selective association of MV^{2+} to the negatively charged colloid interface; $K_{a(298K)} = 140\,000 \pm 20\,000$ M^{-1}. Flash photolysis experiments reveal that only free MV^{2+} is operative in the quenching of $^3Rb^{2-}$; $k_q = 4.7 \pm 1 \times 10^9$ M^{-1}·s^{-1}.

Formation of ground-state donor-acceptor complexes between xanthene dyes and *N*,*N*′-dialkylbipyridinium salts in aqueous and organic solutions is well established.[1-3] In a recent study, the X-ray structures of different complexes of eosin and *N*,*N*′-dialkyl-4,4′-bipyridinium salts were reported.[3] The formation of a 1:1 layered donor-acceptor complex between eosin and *N*,*N*′-dimethyl-4,4′-bipyridinium was established, while a 2:1 crystalline structure between eosin and *N*,*N*′-dibenzyl-4,4′-bipyridinium was formed. In the latter complex structure, one bipyridinium unit is intercalated between two eosin units and a second bipyridnium component is located in an external position to the "sandwich" complex configuration, and acts only in charge neutralization of the assembly. On the basis of the structural characteristics of these complexes, it was concluded that electrostatic interactions as well as π-π donor-acceptor and charge-transfer interactions play important roles in stabilization of these complexes.[3] The structures of eosin-*N*,*N*′-dimethyl-4,4′-bipyridinium complexes in organic solvent were followed too.[3] It has been found that in a DMF solution the initial 1:1 complex is transformed into the thermodynamically stable 2:1 complex ($k = 57.3$ M^{-1}·s^{-1} at 331 K).

The formation of ground-state complexes between xanthene dyes and bipyridinium salts, V^{2+}, prohibits the application of the dyes as effective photosensitizers in light-induced electron-transfer processes:[4] although the electron-transfer quenching of the excited singlet state of the photosensitizer proceeds effectively in the complex configuration, the back electron transfer of the photoproducts in the encounter ion pair cage is rapid, eq 1. Consequently, no separated photoproducts are detectable. In a previous report,[4] we showed that SiO_2 colloids separate ground-state complexes of xanthene dyes-bipyridinium assemblies by means of electrostatic interactions. In such microheterogeneous systems, selective attraction of the bipyridinium component to the negatively charged SiO_2 interface results in the separation of these complexes.

$$dye^{2-} + V^{2+} \rightleftharpoons [dye^{2-}\cdots V^{2+}] \underset{k_b}{\overset{h\nu}{\rightleftharpoons}} [dye^{\bullet-}\cdots V^{\bullet+}] \qquad (1)$$

Here we report on the structure of the Rose Bengal, Rb^{2-} (**1**), and *N*,*N*′-dimethyl-4,4′-bipyridinium, MV^{2+} (**2**), complex and its thermodynamic properties in an aqueous solution. We characterize the separation of the complex in the presence of SiO_2 colloids and reveal the possibility of applying such a process as a means to characterize surface properties of charged colloids. We also follow the photophysical properties of Rose Bengal (**1**) in the presence of MV^{2+} (**2**) in a homogeneous aqueous solution and in a microheterogeneous assembly that includes SiO_2 colloid particles. In this study we highlight the effects of the microheterogeneous assembly on the photophysical properties of the photosensitizer.

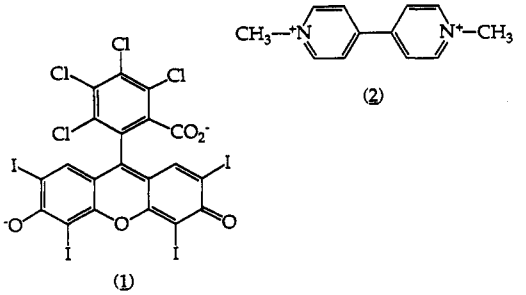

(2)

(1)

† This paper is dedicated to Prof. M. Calvin on the occasion of his 80th birthday.

0022-3654/92/2096-6061$03.00/0

TABLE I: Crystallographic Data for Rose Bengal–Methylviologen Complex

formula	$C_{20}H_2O_5Cl_4I_4 \cdot C_{12}H_{14}N_2 \cdot {}^3/_2H_2O \cdot {}^1/_2CH_3OH$
M	1201
space group	$P2_1/c$
a, Å	20.274 (5)
b, Å	23.168 (5)
c, Å	17.251 (4)
β, deg	106.74 (2)
V, Å^3	7760 (1)
Z	8
ρ(calcd), g cm^{-3}	2.06
μ(Mo Kα), cm^{-1}	32.87
no. of unique reflections	8323
no. of reflections with $I \geq 3\sigma_I$	5650
R	0.052
R_w	0.080
w^{-1}	$\sigma^2_F + 0.001152F^2$

Experimental Section

Purified Rose Bengal (dipotassium salt), Rb^{2-} (**1**), and *N*,*N*′-dimethyl-4,4′-bipyridinium (dichloride), MV^{2+} (**2**), were of commercial source (Aldrich) and were used without further purification. Colloidal SiO_2 (85%, pH 9.3 ± 0.1) was prepared by diluting a commercial 14.5% SiO_2 colloid (mean particle diameter 50 Å, surface area 600 m^2 g^{-1}, particle concentration 1.7×10^{-3} M; Nalco Chemical Co., 2901 Butterfield Rd., Oak Brook, IL 60521).

Absorption spectra were recorded with a UVIKON 860 (Kontron) spectrophotometer equipped with a thermostatic cell holder, where temperature was maintained within ±0.5 K. Association constants and thermodynamic parameters of the complex Rose Bengal–*N*,*N*′-dimethyl-4,4′-bipyridinium, MV^{2+}, were derived from the absorption changes of Rb^{2-}, λ = 542 nm, upon addition of different MV^{2+} concentrations, in a temperature-controlled cuvette (±0.5 K). Laser flash photolysis experiments were performed with a Nd:YAG laser system MY-34-10 (Laser Photonics), linked to a K-347 laser kinetic spectrometer (Applied Photophysics). Transients were recorded and averaged on a 2430 A TEKTRONIX digital oscilloscope, and analyzed by means of an IBM computer. Typically, 16–32 replicate shots were recorded and averaged in each experiment.

Electron-transfer quenching of $^3Rb^{2-}$ by MV^{2+} was followed by means of laser flash photolysis experiments under an argon atmosphere. Aqueous solutions, pH 9.3 ± 0.1, containing Rb^{2-}, 1.4×10^{-5} M, were flashed at λ = 532 nm (generating about 1.5×10^{-6} M $^3Rb^{2-}$) in the presence of different MV^{2+} concentrations and in the presence and absence of 0.85% (w/w) SiO_2 colloid. The lifetime of $^3Rb^{2-}$ was determined from T–T absorption of the dye at λ = 630 nm and the ground-state bleaching at λ = 542 nm.

X-ray crystal structure analyses were performed on a PW1100/20 Philips four-circle computer-controlled diffractometer; Mo Kα (λ = 0.71069 Å) radiation with a graphite crystal monochromator in the incident beam was used. The unit cell dimensions were obtained by a least-squares fit of 24 centered refractions in the range of $10° < \theta < 15°$. Intensity data were collected using the ω–2θ technique to a maximum 2θ of 45°. The scan width, $\Delta\omega$, for each reflection was (1.00 ± 0.35)(tan θ) with a scan speed of 3.0 deg/min. Background measurements were made for a total of 20 s at both limits of each scan. Three standard reflections were monitored every 60 min. No variations in intensities were found. Intensities were corrected for Lorentz and polarization and absorption effect. All non-hydrogen atoms were found by using the results of the SHELXS-86 direct method analysis (Sheldrick, G. M. *Crystallographic Computing 3*; Oxford University Press: Oxford, 1985; pp 175–189). After several cycles of refinements (all crystallographic computing was done on a CYBER 855 computer at the Hebrew University of Jerusalem, using the SHELX 1977 structure determination package) the positions of the hydrogen atoms were calculated, and added with a constant isotropic temperature factor of 0.08 Å^2 to the refinement process. Refinement proceeded to convergence by minimizing the function $\sum w(|F_o| - |F_c|)^2$. A final difference Fourier synthesis map showed several peaks less than 1.0 e/Å^3 scattered about the unit cell without a significant feature. The discrepancy indicates $R = \sum||F_o| - |F_c||/\sum|F_o|$ and $R_w = [\sum w(|F_o| - |F_c|)^2/\sum w(|F_o|)^2]^{0.5}$, which are presented with other pertinent crystallographic data in Table I.

Single crystals of the complexes were obtained by mixing a Rose Bengal aqueous solution with an aqueous solution of methylviologen. The precipitate was filtered, washed with water, and dissolved in a 10:1 (v/v) methanol–water solution. Single crystals were obtained by slow evaporation of the solution. Crystals were sealed in a capillary tube with a drop of the solution for X-ray analysis.

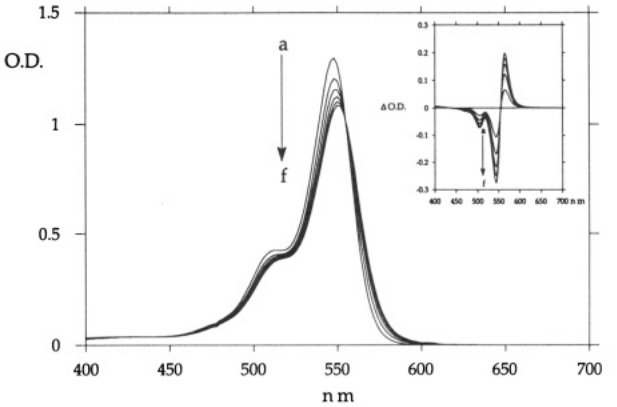

Figure 1. Absorption spectra and differential absorption spectra (inset) of Rose Bengal (**1**), 1.45×10^{-5} M, upon addition of MV^{2+} (**2**): (a) 0, (b) 3.5×10^{-5}, (c) 7×10^{-5}, (d) 1.05×10^{-4}, (e) 1.4×10^{-4}, (f) 1.75×10^{-4} M.

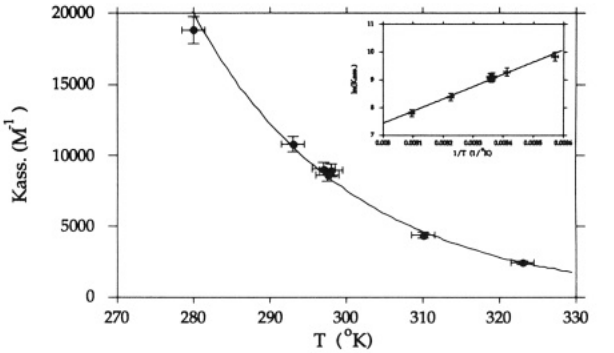

Figure 2. Association constants between Rose Bengal (**1**) and MV^{2+} (**2**) as a function of temperature. Inset shows the plot of ln K_a as a function of $1/T$.

Results and Discussion

Rose Bengal Rb^{2-} (1) and MV^{2+} (2) Complex. Addition of *N*,*N*′-dimethyl-4,4′-bipyridinium, MV^{2+} (**2**), to an aqueous solution of Rb^{2-} (**1**) results in a red shift in the absorption band of the dye, λ = 548 nm, Figure 1. The appearance of one isosbestic point at λ = 555 nm, at different MV^{2+} concentrations, indicates the formation of only one type of complex in the entire concentration range of MV^{2+} used. By assuming a 1:1 complex structure, eq 2, and from the changes in the absorption spectra of Rb^{2-} at

$$Rb^{2-} + MV^{2+} \underset{}{\overset{K_a}{\rightleftharpoons}} [Rb^{2-} \cdots MV^{2+}] \qquad (2)$$

different MV^{2+} concentrations, the association constant, K_a, for the complex is determined using the Benesi–Hildebrand relation.[5] The fact that a linear relationship between $[Rb^{2-}]_o[MV^{2+}]_o/\Delta OD$ and $[Rb^{2-}]_o + [MV^{2+}]_o$, where ΔOD is the absorbance change of the dye upon addition of MV^{2+} and $[Rb^{2-}]_o$ and $[MV^{2+}]_o$ are the analytical concentrations of **1** and **2**, reflects that a 1:1 complex is indeed formed in the aqueous medium. The derived value of the association constant corresponds to K_a(298K) = 9000 ± 500 M^{-1}. By following the association constant K_a at different tem-

TABLE II: Important Bond Lengths (Å) and Angles (deg) for the $Rb^{2-}...MV^{2+}$ Complexes

		1:1 [$Rb^{2-}\cdots MV^{2+}$] Complex			
N1–C31	1.48 (3)	O3–C8	1.28 (2)	I4–C9	2.11 (2)
N2–C32	1.50 (2)	O4–C20	1.26 (2)	Cl1–C16	1.75 (1)
C25–C26	1.47 (2)	O5–C20	1.24 (2)	Cl2–C17	1.74 (2)
O1–C5	1.38 (2)	I1–C2	2.10 (2)	Cl3–C18	1.71 (2)
O1–C6	1.37 (1)	I2–C4	2.07 (2)	Cl4–C19	1.72 (2)
O2–C3	1.23 (2)	I3–C7	2.10 (2)		
	α(C11–C12–C14–C19)		86.21		
	α(C22–C23–C29–C30)		8.96		
		1:2:1 [$Rb^{2-}\cdots MV^{2+}\cdots Rb^{2-};MV^{2+}$] Complex			
N3–C38	1.48 (3)	O2′–C3′	1.26 (2)	I3′–C7′	2.08 (2)
N4–C44	1.52 (3)	O3′–C8′	1.23 (3)	I4′–C9′	2.11 (2)
C37–C37′	1.49 (2)	O4′–C20′	1.29 (3)	Cl1′–C16′	1.74 (1)
C43–C43′	1.50 (3)	O5′–C20′	1.26 (2)	Cl2′–C17′	1.77 (2)
O1′–C5′	1.36 (2)	I1′–C2′	2.10 (2)	Cl3′–C18′	1.72 (2)
O1′–C6′	1.35 (2)	I2′–C4′	2.09 (2)	Cl4′–C19′	1.75 (1)
	α(C11–C12–C14–C19)		85.45		
	α(C22–C21–C21′–C22′)		0.00		
	α(C34–C33–C33″–C34′)		0.00		

TABLE III: Center to Center Interring Distances (Å) in Rose Bengal–Methylviologen Complexes[a]

		[$Rb^{2-}\cdots MV^{2+}$]			
d(3–6)	3.78	α(2–6)	3.33	d(2–NN)	3.46
d(1–5)	>5.00	α(1–5)	4.99	d(3–NN)	3.48
α(3–6)	2.82	d(1–NN)	3.47		
		[$Rb^{2-}\cdots MV^{2+}\cdots Rb^{2-};MV^{2+}$]			
d(1′–5′)	3.70	α(1′–5′)	1.41	d(1′–N3N3′)	3.43
d(2′–5′)	3.84	α(2′–5′)	2.08	d(2′–N3N3′)	3.47
d(3′–5′)	4.27	α(3′–5′)	1.87	d(3′–N3N3′)	3.51

[a] Ring assignment is as follows:

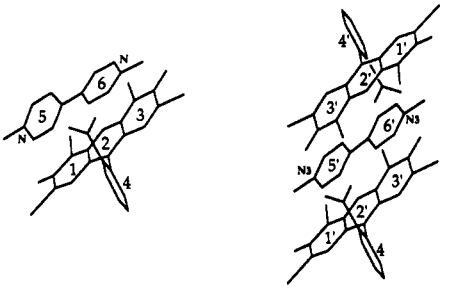

peratures, the thermodynamic parameters associated with the formation of the complex [$Rb^{2-}\cdots MV^{2+}$] were derived and correspond to $\Delta G° = -22.56 \pm 1.1$ kJ·mol^{-1}, $\Delta H° = -36.62 \pm 2$ kJ·mol^{-1}, and $\Delta S = -0.048 \pm 0.0025$ kJ·mol^{-1}, Figure 2.

The single crystal structure of the Rose Bengal–MV^{2+} system reveals unique properties, Figure 3. Table II provides important bond lengths and angles for the two structures while Table III provides the interring distances and angles for the two complexes. The unit cell contains two different types of complexes, Figure 3a: one complex involves a 1:1 structure between Rb^{2-} and MV^{2+}, [$Rb^{2-}\cdots MV^{2+}$], Figure 3b. The bipyridinium component neutralizes the negative charges of Rose Bengal in the complex structure. The dihedral angle between the two pyridinium rings is 8.96°. For comparison, in *N,N′*-dimethylbipyridinium dichloride, MV^{2+}, the dihedral angle between the pyridinium rings corresponds to 0°, and in the complex [$Eo^{2-}\cdots MV^{2+}$] this angle corresponds[3] to 12.13°. In the 1:1 complex we see that one pyridinium ring is almost coplanar with the three-ring plane of the Rose Bengal. The center to center distance between ring 6 of the bipyridinium component and ring 3 of the Rose Bengal is 3.78 Å with an interring angle of 2.82°. This distance and relative orientation are in the range of values observed in other donor–acceptor complexes where π-interactions are operative, and reflect the existence of π-interactions between the two rings.[6,7] The second pyridinium ring (**5**) is deflected by an angle of 4.99° relative to ring 1 of Rose Bengal. The center to center ring distance between

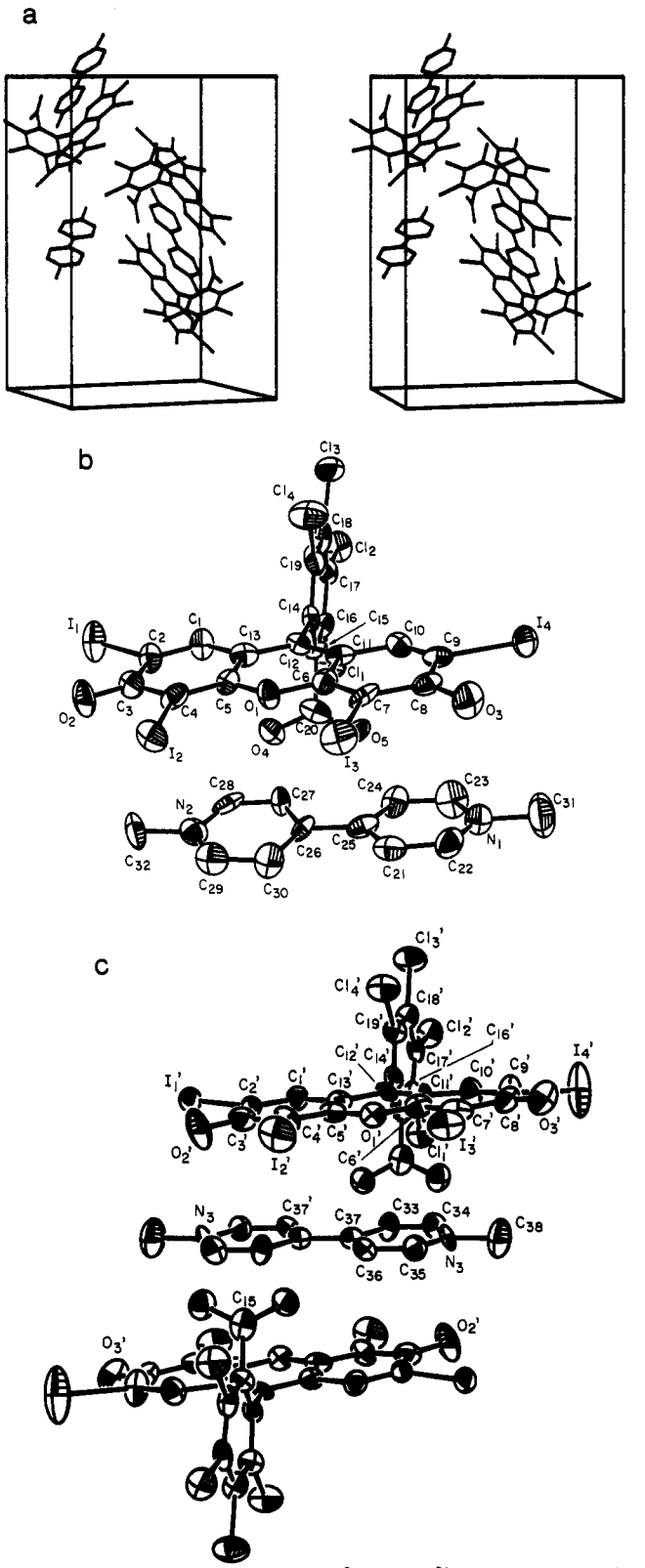

Figure 3. (a) Part of unit cell in the Rb^{2-} and MV^{2+} crystal (stereoscopic view). (b) Structure of the 1:1 [$Rb^{2-}\cdots MV^{2+}$] complex in the crystal. (c) Structure of the 1:2:1 [$Rb^{2-}\cdots MV^{2+}\cdots Rb^{2-};MV^{2+}$] complex in the crystal.

these two rings is more than 5 Å, suggesting the absence of π-interactions between them.

A structurally different complex that coexists in the same unit cell is the 2:1:1 complex [$Rb^{2-}\cdots MV^{2+}\cdots Rb^{2-};MV^{2+}$], Figure 3c. This complex involves the intercalation of a MV^{2+} unit between two Rb^{2-} components while the other MV^{2+} unit is located in an external position to sandwich assembly $Rb^{2-}\cdots MV^{2+}\cdots Rb^{2-}$, and acts only in charge neutralization. It can be seen that in this complex the dihedral angle between the two bipyridinium rings

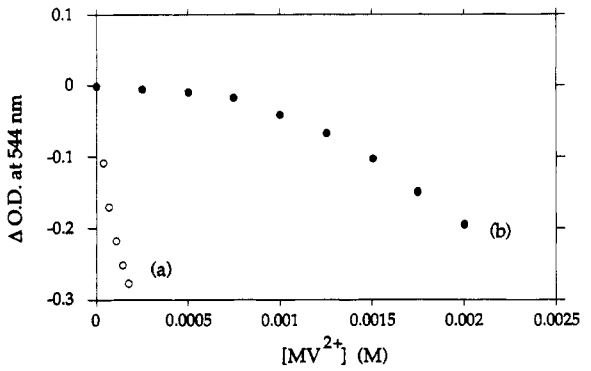

Figure 4. Changes in the absorbance of Rose Bengal (λ = 544 nm) (**1**), 1.45×10^{-5} M, as a function of MV^{2+} (**2**) concentrations: (a) in a homogeneous aqueous solution, pH 9.3 ± 1, and (b) in the presence of 0.85% (w/w) aqueous colloidal silica, pH 9.3 ± 1.

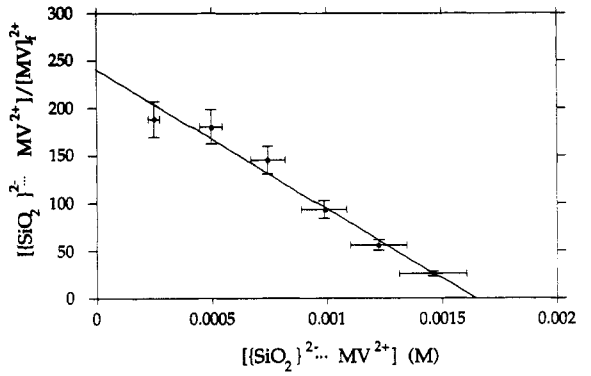

Figure 5. $[\{SiO_2^{2-}\}\cdots MV^{2+}]/[MV^{2+}]_f$ as a function of $[\{SiO_2^{2-}\}\cdots MV^{2+}]$, $[\{SiO_2^{2-}\}\cdots MV^{2+}]$, and $[MV^{2+}]_f$ values were calculated using eqs 4 and 5.

is 0° in the intercalated as well as in the free unit. The $Rb^{2-}\cdots MV^{2+}\cdots Rb^{2-}$ is almost coplanar, and the center to center interring distances between one bipyridinium ring (6′) and rings 1′, 2′, and 3′ of the Rose Bengal unit are 3.70, 3.84, and 4.27 Å, respectively. As the sandwich assembly includes an inversion center, the same distances are found between the second bipyridinium ring (5′) and the rings of the second Rose Bengal component. Thus, this complex consists of eight aromatic rings that are stabilized by interring π–π-interactions. The two complexes coexist in the same unit cell with no apparent intercomplex π–π-interactions or electrostatic interactions.

Separation of $[Rb^{2-}\cdots MV^{2+}]$ Complex by SiO_2 Colloids. In basic aqueous media (pH > 8), SiO_2 colloids are negatively charged as a result of ionization of surface silanol groups.[8] Previous studies have applied the electrical surface potential of SiO_2 particles in controlling photoinduced electron-transfer reactions[9,10] and specifically in the retardation of back-electron-transfer reactions. The negatively charged interface of SiO_2 colloids suggests that this microheterogeneous medium could effect the separation of the ground-state complex $[Rb^{2-}\cdots MV^{2+}]$. By selective attraction of the positively charged component of the complex, MV^{2+}, separation of the complex is anticipated provided that the attractive interactions of MV^{2+} with the SiO_2 interface overcome the stabilizing interactions present in the complex $[Rb^{2-}\cdots MV^{2+}]$.

Addition of the SiO_2 colloid to an aqueous solution that includes Rb^{2-} does not affect its absorption spectrum, indicating that Rb^{2-} does not interact with the SiO_2 colloid. Addition of MV^{2+} to the aqueous Rb^{2-} solution results in a red shift and absorbance decrease in the Rb^{2-} spectrum, Figure 4a, as a result of formation of the ground-state complex $[Rb^{2-}\cdots MV^{2+}]$. Addition of the SiO_2 colloid to the aqueous solution of the complex $[Rb^{2-}\cdots MV^{2+}]$ restores the absorption band of free Rb^{2-}. Similarly, addition of MV^{2+} to an aqueous SiO_2 colloid that includes Rb^{2-} results in substantially smaller changes in the absorbance of Rb^{2-} as compared to those occurring in the homogeneous solution, Figure 4b. These results clearly indicate that addition of the SiO_2 colloid to the solution of the complex $[Rb^{2-}\cdots MV^{2+}]$ effects its separation and that the formation of the complex is substantially retarded in the microheterogeneous system. These results are in accordance with the original suggestion, where association of MV^{2+} to the negatively charged SiO_2 interface is anticipated to separate the ground-state complex $[Rb^{2-}\cdots MV^{2+}]$ or eliminate its formation.

Thus, in an aqueous SiO_2 colloid that includes Rb^{2-} and MV^{2+} two equilibrium processes are operative, eq 3: (i) an equilibrium that generates the ground-state complex $[Rb^{2-}\cdots MV^{2+}]$ and (ii) an equilibrium process where MV^{2+} is associated with the SiO_2 interface. The association constants for these two processes K_1

$$[\{SiO_2\}^{2-}\cdots MV^{2+}] + Rb^{2-} \underset{\{SiO_2\}^{2-}}{\overset{K_2}{\rightleftharpoons}} Rb^{2-} + MV^{2+} \overset{K_1}{\rightleftharpoons} [Rb^{2-}\cdots MV^{2+}] \quad (3)$$

and K_2, respectively, are given in eqs 4 and 5 where $[Rb^{2-}]_a$ and $[\{SiO_2\}^{2-}]_a$ are the analytical concentrations of Rb^{2-} and the negatively charged SiO_2 binding sites, respectively, and $[MV^{2+}]_f$ is the concentration of free MV^{2+} in the presence of Rb^{2-} and the SiO_2 colloid.

$$K_1 = [Rb^{2-}\cdots MV^{2+}]/(([Rb^{2-}]_a - [Rb^{2-}\cdots MV^{2+}])[MV^{2+}]_f) \quad (4)$$

$$K_2 = [\{SiO_2\}^{2-}\cdots MV^{2+}]/((([\{SiO_2\}^{2-}]_a - [\{SiO_2\}^{2-}\cdots MV^{2+}])[MV^{2+}]_f) \quad (5)$$

Equation 5 can be rearranged into eq 5a, and $[MV^{2+}]_f$ and $[\{SiO_2\}^{2-}\cdots MV^{2+}]$ can be expressed by eqs 4a and 5b, respectively. Thus, plotting $[\{SiO_2\}^{2-}\cdots MV^{2+}]/[MV^{2+}]_f$ as a function of $[\{SiO_2\}^{2-}\cdots MV^{2+}]$, where $[MV^{2+}]_f$ and $[\{SiO_2\}^{2-}\cdots MV^{2+}]$ are calculated using eqs 4a and 5b, respectively, gives K_2 (the association constant of MV^{2+} to the SiO_2 colloid) as the slope and $K_2[\{SiO_2\}^{2-}]_a$ as the intercept (eq 5a).

$$[\{SiO_2\}^{2-}\cdots MV^{2+}]/[MV^{2+}]_f = K_2[\{SiO_2\}^{2-}]_a - K_2[\{SiO_2\}^{2-}\cdots MV^{2+}] \quad (5a)$$

$$[MV^{2+}]_f = [Rb^{2-}\cdots MV^{2+}]/([Rb^{2-}]_a - [Rb^{2-}\cdots MV^{2+}])K_1 \quad (4a)$$

$$[\{SiO_2\}^{2-}\cdots MV^{2+}] = [MV^{2+}]_a - [MV^{2+}]_f - [Rb^{2-}\cdots MV^{2+}] \quad (5b)$$

Following this analysis, the extent of formation of the complex $[Rb^{2-}\cdots MV^{2+}]$ in the presence of Rb^{2-} and the SiO_2 colloid has been determined. To an aqueous solution of Rb^{2-}, 1.45×10^{-5} M that includes 0.85% (w/w) SiO_2 colloid, corresponding to 1.0×10^{-4} M in SiO_2 particles, is added MV^{2+}, Figure 5. From the changes in the absorption spectrum of Rb^{2-} (ΔOD), and knowing the association constant K_1 (vide supra), the concentration of the complex $[Rb^{2-}\cdots MV^{2+}]$ and $[MV^{2+}]_f$ at each concentration of added MV^{2+} are determined. These values are introduced into eqs 4a and 5b, and the plot according to eq 5a is shown in Figure 6. The derived value of K_2 is $K_2 = 140000 \pm 20000$ M^{-1}. This analysis assumes that each MV^{2+} unit binds to two ionized silanol groups, and that binding of MV^{2+} to the SiO_2 surface is not affected by already surface associated MV^{2+}. We thus realize that the association of MV^{2+} to the SiO_2 particles is substantially stronger than the association constant of the complex $[Rb^{2-}\cdots MV^{2+}]$. Therefore, the SiO_2 colloid separates the complex, and one can assume that at low concentrations of MV^{2+} the dye Rb^{2-} is essentially in its free form.

Futhermore, assuming that each binding site of MV^{2+} to the colloid interface involves two negative SiO_2 charges (two ionized silanol groups) allows us to characterize the surface properties of the SiO_2 colloid. From the intercept of the plot shown in Figure 5 the analytical concentration of SiO_2 binding sites is found to correspond to $[\{SiO_2\}^{2-}] = 2.2 \times 10^{-3}$ M. As the particle concentration of the SiO_2 colloid is 1.0×10^{-4} M one can deduce that each particle bears 22 ± 3 binding sites (or 44 ± 6 ionized groups).

Photophysical Properties of Rb^{2-} in the Presence of MV^{2+}. The quantum yield of triplet state formation of Rose Bengal formation, $^3Rb^{2-}$, corresponds to $\phi_T = 0.76$[11], and its lifetime is $\tau = 43.6$ μs. Table IV summarizes the effect of added MV^{2+} on the fluorescence quantum yield and lifetime in a homogeneous phase and in the

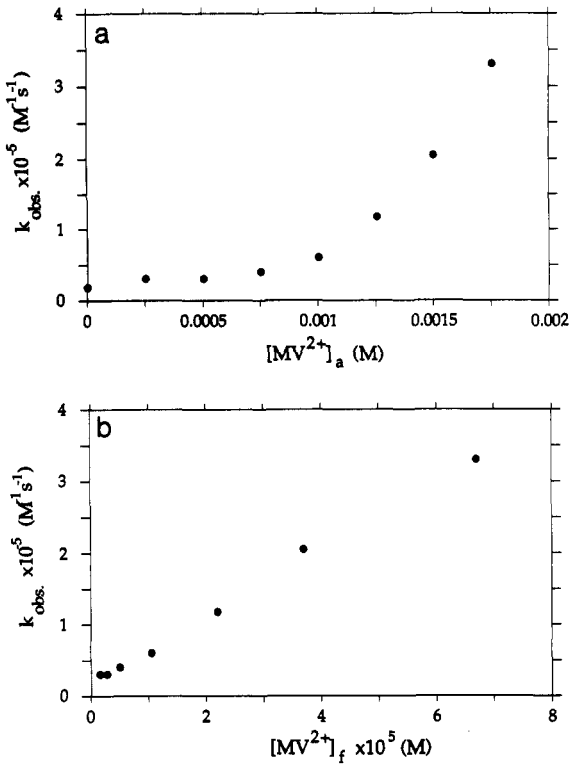

Figure 6. Observed rate constant for quenching of $^3Rb^{2-}$ by MV^{2+} (2) in the presence of 0.85% (w/w) aqueous colloidal silica, pH 9.3 ± 1: (a) k_{obs} plotted as a function of the analytical concentration of MV^{2+} in solution and (b) k_{obs} plotted as a function of the concentration of free MV^{2+} in solution.

microheterogeneous SiO_2 system. For clarity, the concentrations of free MV^{2+}, $[MV^{2+}]_f$ and free Rb^{2-}, $[Rb^{2-}]_f$ in each of the systems are also included in Table IV. These values are calculated using K_1 and K_2. It is evident that, in the homogeneous aqueous system, addition of small concentrations of MV^{2+} decreases the quantum efficiency for the formation of $^3Rb^{2-}$ and simultaneously shortens its lifetime. For example, in the presence of $[MV^{2+}] = 5.14 \times 10^{-5}$ M, the quantum efficiency for the triplet formation drops from $\phi_T = 0.76$ to $\phi_T = 0.533$ and its lifetime is shortened to 1.35 μs.

The quantum efficiency of $^3Rb^{2-}$ correlates nicely with the concentration of free Rb^{2-} available in the presence of MV^{2+}. Thus, the decrease in the quantum yield, ϕ_T, in the homogeneous aqueous solution is attributed to the formation of the complex $[Rb^{2-}\cdots MV^{2+}]$. In this assembly, the excited singlet state, Rb^{2-}, is statically quenched by MV^{2+} and interconversion to the triplet state is eliminated. From the decrease in the lifetime of $^3Rb^{2-}$ upon addition of MV^{2+}, the quenching rate constant, eq 6, is derived and corresponds to $k_q = (1.5 \pm 0.2) \times 10^{10}$ $M^{-1}\cdot s^{-1}$.

$$^3Rb^{2-} + MV^{2+} \xrightarrow{k_q} Rb^{\bullet-} + MV^{\bullet+} \qquad (6)$$

In the presence of the SiO_2 colloid, the quantum efficiency of the triplet state $^3Rb^{2-}$ is substantially enhanced in the presence of MV^{2+} (Table IV). For example, in the presence of $[MV^{2+}] = 1 \times 10^{-3}$ M and the SiO_2 colloid, ϕ_T corresponds to 0.695, while in the homogeneous phase, under similar conditions, ϕ_T drops to the value 0.1. It is also evident from Table IV that although the quantum efficiency of ϕ_T remains high in the presence of MV^{2+}, in the microheterogeneous system the lifetime τ_T is shortened. Figure 6a shows the observed decay rate constant of the triplet state, k_{obs}, as a function of MV^{2+} concentration added to the system. It is evident that, at low MV^{2+} concentrations, the triplet state is ineffectively quenched, and its lifetime (or decay rate constant) is almost unaffected. When $[MV^{2+}]$ reaches the value of ca. 1.0×10^{-3} M, a sharp enhancement in the decay process of $^3Rb^{2-}$ is observed. It seems reasonable to assume that $^3Rb^{2-}$, being negatively charged and repelled by the SiO_2 colloid, interacts only with free MV^{2+}. Thus, we analyzed the nonlinear quenching process of $^3Rb^{2-}$ in terms of free quencher $[MV^{2+}]_f$. Knowing the value of K_2, the association constant of MV^{2+} to the SiO_2 particles, and K_1, the association constant of the complex $[Rb^{2-}\cdots MV^{2+}]$, the concentration of free MV^{2+} at each analytical concentration of added MV^{2+} can be calculated, Table IV. Figure 6b shows the decay rate constants of $^3Rb^{2-}$ as a function of free MV^{2+} concentration, $[MV^{2+}]_f$, for the systems exhibiting the macroscopic nonlinear quenching behavior. It is evident that a linear Stern–Volmer plot is obtained, Figure 6b. Thus, the nonlinear quenching of $^3Rb^{2-}$ in the SiO_2 colloid originates from the association of MV^{2+} to the colloid interface: The dye Rb^{2-} is negatively charged and therefore repelled from the colloid interface. At low concentrations of added MV^{2+}, most of the electron acceptor is attracted by the SiO_2 colloid (Table IV) and the concentration of free MV^{2+} is low. Consequently, the quenching of $^3Rb^{2-}$ is inefficient. When the concentration of MV^{2+} is further increased, K_1 and K_2 imply that the concentration of free MV^{2+} will sharply increase, and as a result a steep enhancement in the quenching rate of $^3Rb^{2-}$ will occur. From the linear Stern–Volmer plot, Figure 6b, the quenching rate constant of $^3Rb^{2-}$ by free MV^{2+}, eq 6, is derived and corresponds to $k_q(SiO_2) = 4.7 \pm 1 \times 10^9$ $M^{-1}\cdot s^{-1}$.

TABLE IV: Triplet Quantum Yields and Lifetimes of Photoexcited Rb^{2-} in the Absence and Presence of MV^{2+} in a Homogeneous Phase and in the Presence of 1% Silica Colloid

	$[MV^{2+}]_{anal.}$, M	$[MV^{2+}]_f$, M	$[Rb^{2-}]_f$,[a] M	Φ_T[b]	τ_T[c]
homogeneous	0	0	1.40×10^{-5}	0.760	43.56
	1.08×10^{-6}	9.59×10^{-7}	1.39×10^{-5}	0.745	44.09
	2.16×10^{-6}	1.92×10^{-6}	1.38×10^{-5}	0.749	25.36
	3.23×10^{-6}	2.88×10^{-6}	1.36×10^{-5}	0.738	21.03
	5.37×10^{-6}	4.79×10^{-6}	1.34×10^{-5}	0.727	13.33
	1.07×10^{-5}	9.58×10^{-6}	1.29×10^{-5}	0.700	6.62
	5.14×10^{-5}	4.73×10^{-5}	9.82×10^{-6}	0.533	1.35
	1.00×10^{-3}	9.87×10^{-4}	1.42×10^{-6}	0.078	
heterogeneous	0	0	1.40×10^{-5}	0.760	36.63
	2.50×10^{-4}	1.32×10^{-6}	1.36×10^{-5}	0.738	32.89
	5.00×10^{-4}	2.76×10^{-6}	1.34×10^{-5}	0.727	31.75
	7.50×10^{-4}	4.83×10^{-6}	1.33×10^{-5}	0.722	23.81
	1.00×10^{-3}	1.06×10^{-5}	1.28×10^{-5}	0.695	16.61
	1.25×10^{-3}	2.20×10^{-5}	1.20×10^{-5}	0.651	12.16
	1.50×10^{-3}	3.69×10^{-5}	1.10×10^{-5}	0.597	4.83
	1.75×10^{-3}	6.69×10^{-5}	9.50×10^{-6}	0.516	3.02
	2.00×10^{-3}	1.00×10^{-4}	8.23×10^{-6}	0.447	1.41

[a] Rose Bengal analytical concentration is 1.4×10^{-5} M in all systems. [b] Calculated assuming that Φ_T(Rose Bengal) = 0.76 and Φ_T(complex) = 0. [c] τ is given in microseconds.

Conclusions

We have highlighted structural features of Rb^{2-} and MV^{2+} complexes and established the thermodynamic parameter associated with the 1:1 complex $[Rb^{2-}\cdots MV^{2+}]$. The structural features of the complex suggest that electrostatic interactions as well as π–π-interactions and donor–acceptor interactions influence the stability of the complex. In aqueous media, the formation of the complex leads to intercomplex electron-transfer quenching of $^1Rb^{2-}$, and the formation of $^3Rb^{2-}$ is inefficient.

In the presence of the microheterogeneous SiO_2 colloid, separation of the donor–acceptor complex $[Rb^{2-}\cdots MV^{2+}]$ occurs due to the selective association of MV^{2+} to the negatively charged SiO_2 interface. Characterization of MV^{2+} association to the SiO_2 particles reveals that the electrostatic attractive interactions between MV^{2+} and the colloid are sufficiently high to overcome the stabilizing interactions operative in the complex $[Rb^{2-}\cdots MV^{2+}]$. Separation of this ground-state complex leads to effective formation of $^3Rb^{2-}$ in the presence of MV^{2+} in the microheterogeneous assembly that includes MV^{2+}. We deduce that only the free electron acceptor $[MV^{2+}]_f$ participates in the electron-transfer quenching of $^3Rb^{2-}$.

Acknowledgment. This research was supported by The Fund for Basic Research administered by the Israel Academy of Science

and Humanities (I.W.) and by the Office of Basic Energy Sciences, Division of Chemical Science, U.S. Department of Energy, under Contract DE-AC02-83CH 10093 (A.J.F.).

References and Notes

(1) (a) Usui, Y.; Misawa, H.; Sakuragi, H.; Tokumaru, K. *Bull. Chem. Soc. Jpn.* **1987**, *60*, 1573. (b) Usui, Y.; Sasaki, Y.; Ishii, Y.; Tokumaru, K. *Bull. Chem. Soc. Jpn.* **1988**, *61*, 3335.
(2) (a) Willner, I.; Eichen, Y.; Marx, S.; Doron, A. *Isr. J. Chem.*, in press. (b) Willner, I.; Marx, S.; Eichen, Y. *Angew. Chem., Int. Ed. Engl.*, in press.
(3) Willner, I.; Eichen, Y.; Rabinovitz, M.; Hoffman, R.; Cohen, S. *J. Am. Chem. Soc.* **1992**, *114*, 637.
(4) Willner, I.; Eichen, Y.; Joselevich, E. *J. Phys. Chem.* **1990**, *94*, 3092.
(5) Benesi, H. A.; Hildebrand, J. H. *J. Am. Chem. Soc.* **1949**, *71*, 2703.
(6) (a) Hunter, C. A.; Sanders, J. K. M. *J. Am. Chem. Soc.* **1990**, *112*, 5525. (b) Price, S. L.; Stone, A. J. *J. Chem. Phys.* **1987**, *86*, 2859. (c) Rigby, M.; Smith, E. B.; Wakeham, W. A.; Maitland, G. C. *The Forces Between Molecules*; Clarendon: Oxford, 1986. (d) *Intermolecular Interactions: From Diatomics to Biopolymers*; Pullman, B., Ed.; Wiley: Chichester, 1978. (e) Fersht, A. R. *Enzyme Structure and Mechanism*; Freeman: New York, 1985.
(7) (a) Foster, L. *Organic Charge-Transfer Complexes*; Academic Press: New York, 1969; Chapters 2 and 8. (b) Nakamura, K.; Kai, Y.; Yasuoka, N.; Kasai, N. *Bull. Chem. Soc. Jpn.* **1981**, *61*, 3300. (c) Kisch, H.; Fernandez, A.; Wakatsuki, Y.; Yamazaki, H. *Z. Naturforsch.* **1985**, *40b*, 292. (d) Bent, H. A. *Chem. Rev.* **1968**, *68*, 587. (e) Megehee, E. G.; Johnson, C. E.; Eisenberg, R. *Inorg. Chem.* **1989**, *28*, 2423. (f) Reddington, M. V.; Slawin, A. M. Z.; Spencer, N.; Stoddart, F. J.; Vicent, V.; Williams, D. J. *J. Chem. Soc., Chem. Commun.* **1991**, 630. (g) Ashton, P. R.; Brown, C. L.; Chrystal, J. T.; Goodnow, T. T.; Kaifer, A. E.; Parry, K. P.; Philip, D.; Slawin, A. M. Z.; Spencer, N.; Stoddart, F. J.; Vicent, V.; Williams, D. J. *J. Chem. Soc., Chem. Commun.* **1991**, 634.
(8) *The Chemistry of Silica*; Iler, R. K., Ed.; Wiley: New York, 1979.
(9) (a) Willner, I.; Degani, Y. *J. Chem. Soc., Chem. Commun.* **1982**, 761. (b) Willner, I., Degani, Y. *J. Am. Chem. Soc.* **1983**, *105*, 6228. (c) Furlong, D. N.; Johansen, O.; Launikonis, A.; Loder, J. W.; Mav, A. W. H.; Sasse, W. H. F. *Aust. J. Chem.* **1985**, *38*, 363.
(10) (a) Willner, I.; Otvos, J. W.; Calvin, M. *J. Am. Chem. Soc.* **1981**, *103*, 3202. (b) Laane, C.; Willner, I.; Otvos, J. W.; Calvin, M. *Proc. Natl. Acad. Sci. U.S.A.* **1981**, *78*, 5928. (c) Willner, I.; Yang, J.-M.; Otvos, J. W.; Calvin, M. *J. Phys. Chem.* **1981**, *85*, 3277.
(11) Valdes-Aguilera, O.; Neckers, D. C. *Acc. Chem. Res.* **1989**, *22*, 171.

Primary Photochemical Events in Halorhodopsin Studied by Subpicosecond Time-Resolved Spectroscopy

Hideki Kandori, Keitaro Yoshihara,*

Institute for Molecular Science, Myodaiji, Okazaki 444, Japan

Hiroaki Tomioka, and Hiroyuki Sasabe

Frontier Research Program, RIKEN (The Institute of Physical and Chemical Research), Hirosawa, Wako, 351-01, Japan *(Received: December 2, 1991; In Final Form: March 6, 1992)*

Primary photochemical events of the light-driven chloride-pump halorhodopsin (hR) are studied at room temperature by subpicosecond transient absorption measurements. On excitation of hR with a 600-nm, 0.6-ps pulse, excited-state absorption and stimulated emission appear immediately in the 420–530-nm and 650–770-nm wavelength regions, respectively, and both decay with a time constant of 2.3 ps. The calculated absorption spectrum of the excited state of hR (hR*) has a peak at 516 nm and a shoulder at about 460 nm. Accompanied by the decay of hR*, the primary ground-state product appears at around 645 nm. The quantum yield of the product formation is determined to be 0.27. The detailed analysis of the kinetics at 645 nm provided the faster rise time of the product ($\leq$1.0 ps) than the decay of the excited state (2.3 ps), as well as the possible presence of the J-intermediate (hR_J). Instead of the simple sequential kinetic model considering three states of hR*, hR_J, and hR, which has been applied to the primary process of bacteriorhodopsin, a parallel channel model is suggested for the primary process of hR. After Franck–Condon excitation, the cis–trans isomerization to hR_J and the relaxation to hR* take place simultaneously. The latter decays only to hR via radiative and nonradiative processes. The present results suggest that the excited state having a reaction channel to cis–trans isomerization is not located at the potential minimum of hR* and that the relaxation process in the excited state is a process in competition with isomerization.

Introduction

Halobacterium halobium contains the four retinal proteins: bacteriorhodopsin (bR), halorhodopsin (hR), sensoryrhodopsin (sR), and phoborhodopsin (pR). bR and hR work for energy generation by light-driven proton and chloride pumps, respectively,[1,2] while sR and pR work for positive and negative phototaxis, respectively.[3,4] Structural varieties and their relationship to the respective functions have been of much interest. Since a photon triggers reactions in each pigment, photochemical reactions of the pigments must be closely related to the functions of the pigments. Flash photolysis experiments on these retinal proteins have mainly focused on bR. In particular, recent developments in ultrashort pulse generation have enabled us to look directly at the relaxation processes in the excited state of the retinal proteins. A number of time-resolved studies on bR have given pictures on cis–trans isomerization in protein.[5-11] According to these studies, the excited state of bR (bR*) depopulates and the first ground-state product J appears with the same rate constant of about $(0.5\ ps)^{-1}$. Since the J-intermediate has a 13-cis-like configuration,[12-14] it has been concluded that cis–trans isomerization occurs along the reaction coordinates in the excited state.

Because it is less convenient to prepare samples, few studies by time-resolved spectroscopy have been made on either hR, sR, or pR. One may tend to consider that the primary photochemical events of these three pigments are same as that of bR. In 1985, however, Polland et al. reported that the lifetime of the excited state of hR (hR*) is 10-times longer (5 ps) than that of bR*.[15] Although both hR and bR have the same chromophore and similar protein environments,[16] the primary reaction rates are 1-order of magnitude different. Thus we have started to investigate the primary photochemical events of hR by use of subpicosecond transient absorption spectroscopy. In a previous paper, we reported the absorption spectrum of hR* which displayed a unique profile.[17] In the present article, we measure the transient absorption spectra of hR and investigate its primary photochemical events. The results obtained strongly imply that the primary process in hR cannot be described by the simple scheme which has been applied to bR.

Materials and Methods

The hR sample was prepared as described previously.[17] A bacteriorhodopsin-deficient strain, OD2, was grown in a 20-L

0022-3654/92/2096-6066$03.00/0